

# Effect of the heat treatment on the microstructure and properties of tin babbitt

B. Leszczyńska-Madej<sup>1\*</sup>, M. Madej<sup>2</sup>

<sup>1</sup>*AGH University of Science and Technology, Faculty of Non-Ferrous Metals, Mickiewicza 30 Av., Kraków, Poland*

<sup>2</sup>*AGH University of Science and Technology, Faculty of Metal Engineering and Industrial Computer Science, Mickiewicza 30 Av., Kraków, Poland*

Received 12 December 2011, received in revised form 28 September 2012, accepted 30 October 2012

## Abstract

The analysis of the microstructure and properties of the tin babbitt SnSb12Cu6Pb after heat treatment is presented in this article.

The specimens were annealed in the conditions: 100°C and 200°C during 2 h and subsequently tested for Brinell hardness, bending strength and wear resistance. The wear tests were carried out using the block – on ring tester. The samples were also investigated by means of both light microscopy (LM) and scanning electron microscopy (SEM).

**Key words:** babbitt, annealing, microstructure, properties, wear resistance

## 1. Introduction

The most popular bearing alloys are based on tin and lead. They are widely used in friction assemblies (e.g., in turbines, compressors, transport, cars and various friction units). These alloys are made of plastic matrix and load bearing particles dispersed in the matrix, which guarantee great abrasion resistance [1–8]. The most advantageous properties point at alloys based on tin containing: 7–13 % Sb, 3–7 % Cu and up to the 1.2 % Cd called babbitt tin according to PN-ISO 4381:1997. The properties of the babbitt considerably depend on its chemical composition and structural state. Treatment of a material causes its structural changes and affects physical and mechanical properties [6].

Data available in literature on the babbitt with high amount of tin show that they can contain three phases:  $\alpha$ ,  $\beta$ ,  $\eta$  or  $\alpha$ ,  $\beta$ ,  $\varepsilon$ . The basic  $\alpha$ -phase can be present in the form of solid solution of antimony and copper in tin or in the form of three-component eutectic [6]. The phase diagrams for the Sn-Sb and Cu-Sn systems are presented in Fig. 1.

As was mentioned above, bearing alloys are widely used in friction assemblies, thus its property of wear resistance is very important. This property is condi-

tioned by the amount and morphological size of the hard phases presented in the alloy, especially SnSb ( $\beta$ ) and CuSn ( $\eta$ ). When hard phases are well refined, the wear resistance of the alloy is enhanced. There are data in the literature illustrating the fact that both fatigue strength [2] and wear resistance [2–4] depend considerably on the material structural state. The heat treatment is one of widespread methods of forming the regulated material structures [9]. For this purpose, the influence of different heat treatment conditions on the babbitt microstructure, plasticity, and wear resistance indices were estimated.

The main object of this study is to determine the influence of the heat treatment on the microstructure and properties of the bearing babbitt SnSb12Cu6Pb.

## 2. Experimental procedure

The investigations were carried out on the tin babbitt alloy SnSb12Cu6Pb. The chemical composition of the high-tin SnSb12Cu6Pb antifricition alloy is given in Table 1.

The samples were annealed in conditions presented below:

– heating in the furnace chamber to the temperat-

\*Corresponding author: tel.: +48 12 617 35 73; e-mail address: [bleszcz@agh.edu.pl](mailto:bleszcz@agh.edu.pl)

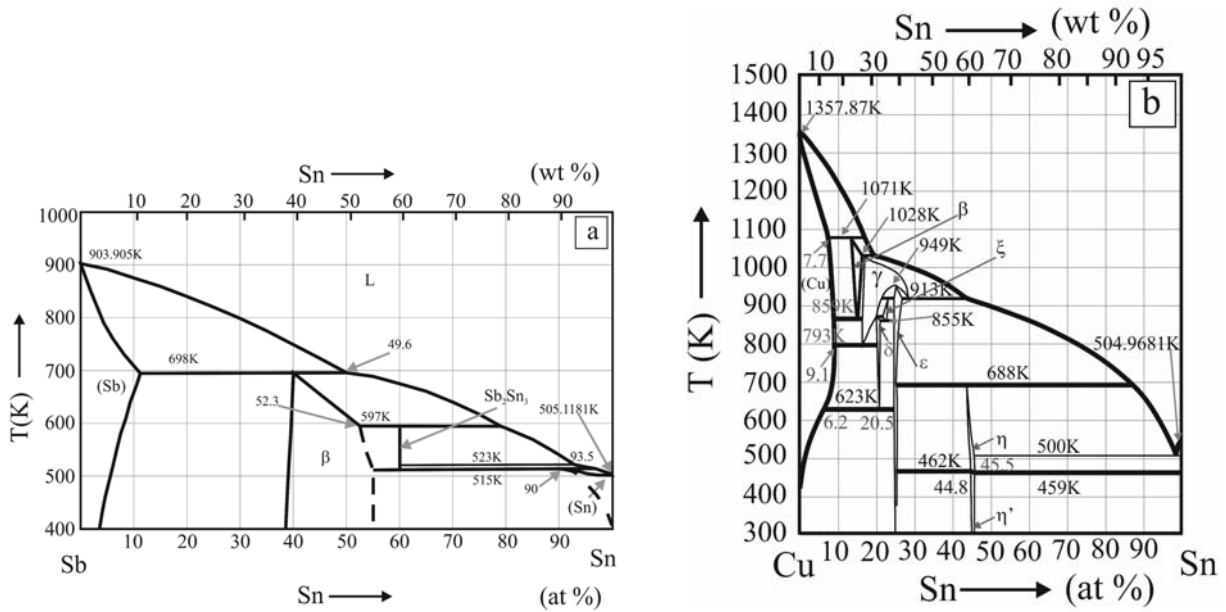


Fig. 1. Phase diagrams: Sn-Sb (a), Cu-Sn (b) [9].

Table 1. Chemical composition of babbitt alloy (wt.%)

Sn	Sb	Cu	Cd	Pb	As	Bi	Fe	Zn
Bal.	11.1	5.97	0.001	0.009	0.002	0.002	0.001	0.003

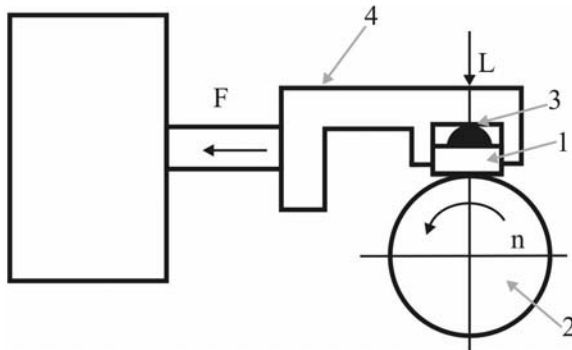


Fig. 2. Schematic view of block-on-ring tester.

ures: 100 °C and 200 °C with the rate 15 °C min<sup>-1</sup>,  
 – isothermal annealing at the temperatures: 100 °C and 200 °C during 2 h,  
 – cooling in the furnace cooler to the ambient temperature.

The specimens were subsequently tested for Brinell hardness, microhardness, bending strength and wear resistance. They were also analyzed by means of both light microscopy (LM) and scanning electron microscopy (SEM). The wear tests were carried out using the block-on-ring tester (Fig. 2).

The sample (1) was mounted in a sample holder (4) equipped with a hemispherical insert (3) ensuring proper contact between the sample and a rotating ring (2). The wear surface of the sample was perpendicular to the pressing direction. Double lever system input the load *L*, pressing the sample to the ring with the accuracy of ±1 %. The ring rotated with a constant rotating speed.

The oil for the wear resistance examination was charged from the steam TK – 120 turbines TG – 8 during turbine operation.

The wear tests conditions chosen for the current investigations were following:

- tested samples: rectangular specimens 20 × 4 × 4 mm<sup>3</sup>,
- counterpart (rotating ring): φ 49.5 × 8 mm<sup>2</sup>, heat treated steel, 55 HRC,
- wet sliding,
- rotational speed: 136 rev min<sup>-1</sup>,
- load: 67 N,
- sliding distance: 1000 m, 10000 m.

The measured parameters were:

- loss of sample mass,
- friction force *F* (used to calculate the friction coefficient).

This tester enabled performing tests in accordance with the methods determined in ASTM D 2714, D 3704, D 2981 and G 77 Standards. The tests were performed under conditions of dry and fluid friction with using the following cooling – separating medium. The friction investigations with application of a lubrication medium started under a dry friction condition.

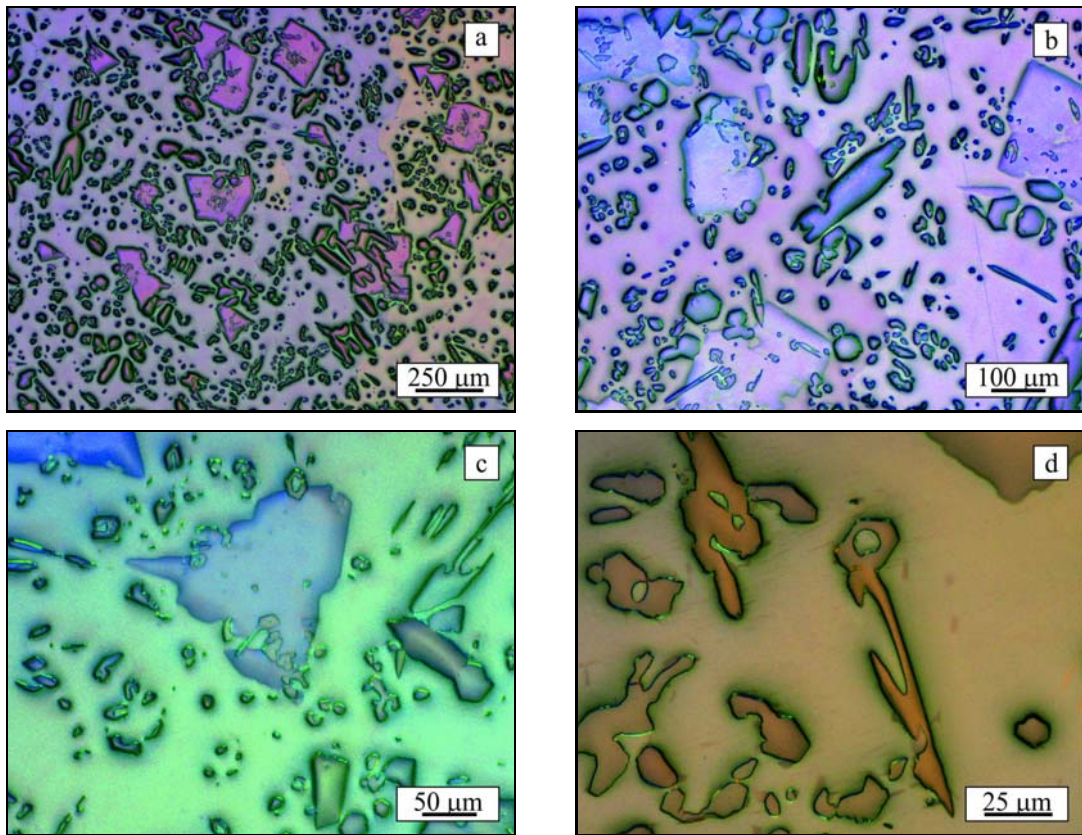


Fig. 3. Microstructures of the babbitt ingot (B83): 50× (a), 100× (b), 200× (c), 500× (d).

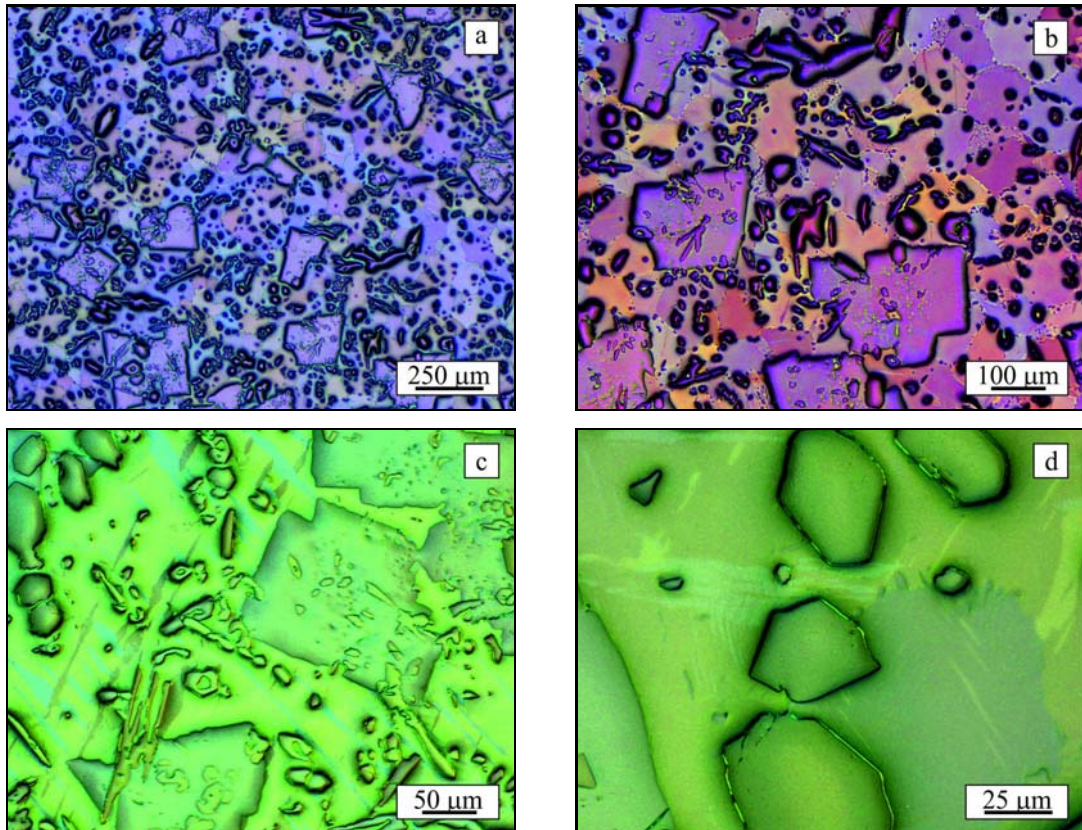


Fig. 4. Microstructures of the annealed at 100°C babbitt (B83): 50× (a), 100× (b), 200× (c), 500× (d).

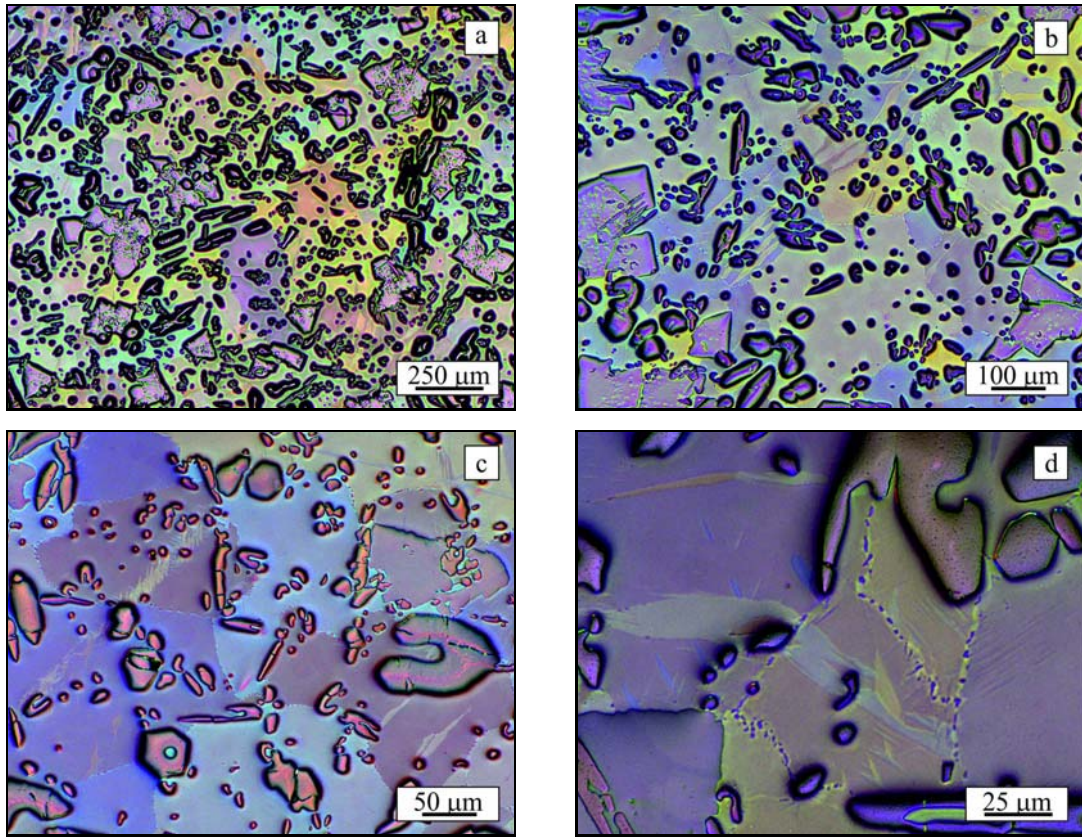


Fig. 5. Microstructures of the annealed at 200°C babbitt (B83): 50× (a), 100× (b), 200× (c), 500× (d).

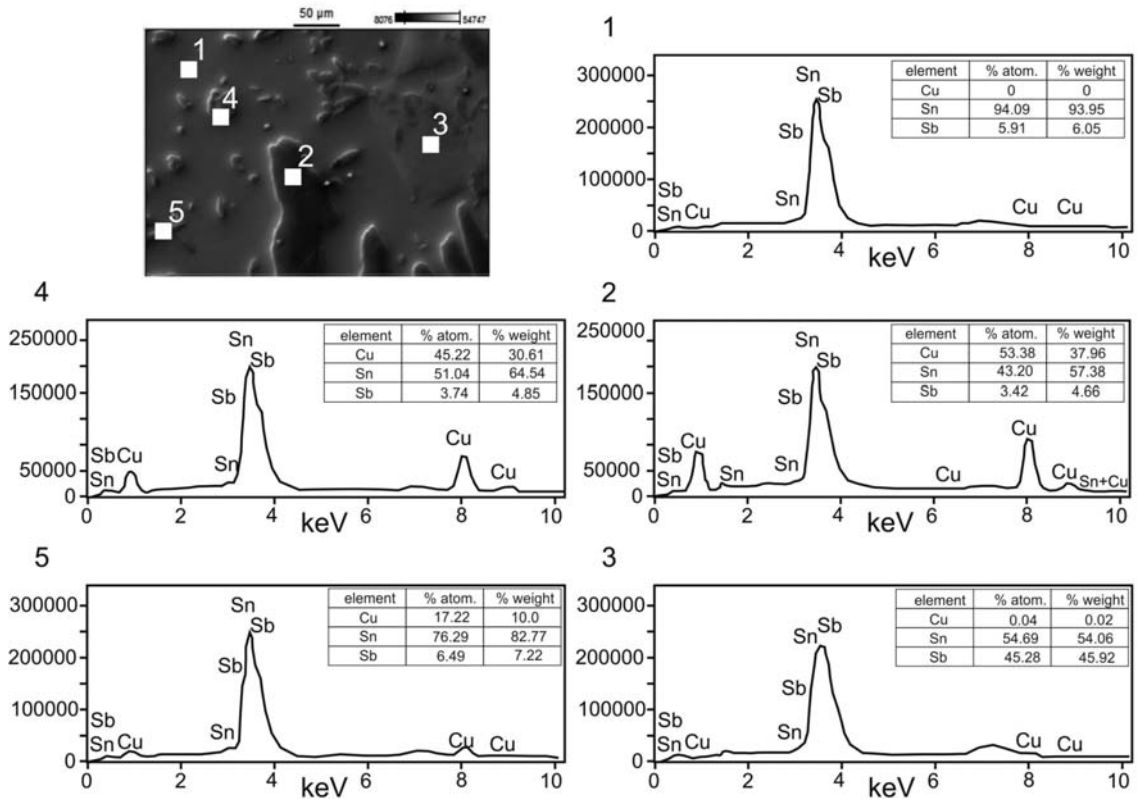


Fig. 6. Microstructure and chemical composition of the phases presented in the babbitt ingot (B83).

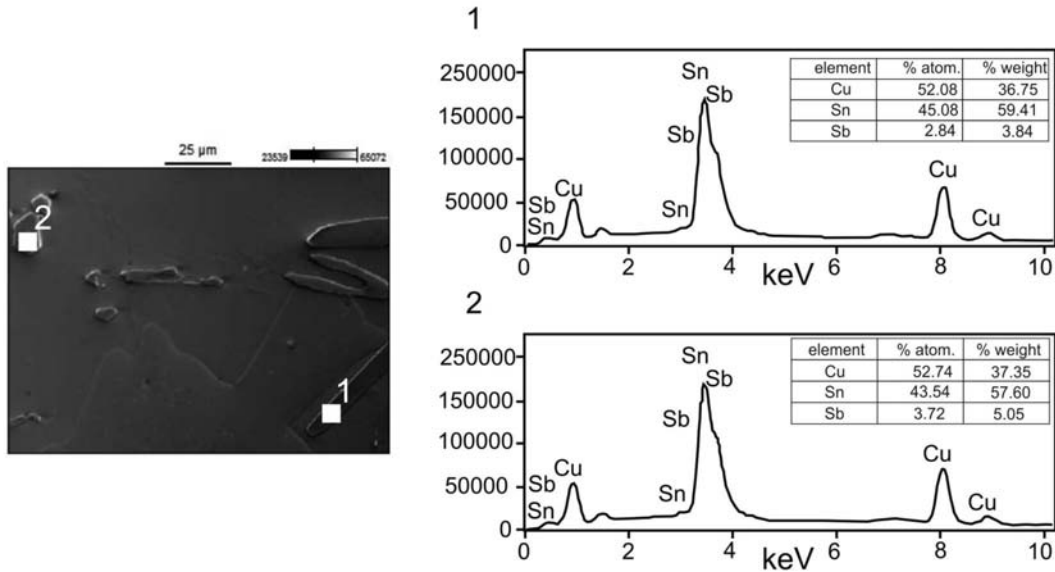


Fig. 7. Microstructure and chemical composition of the phases presented in the babbitt ingot (B83).

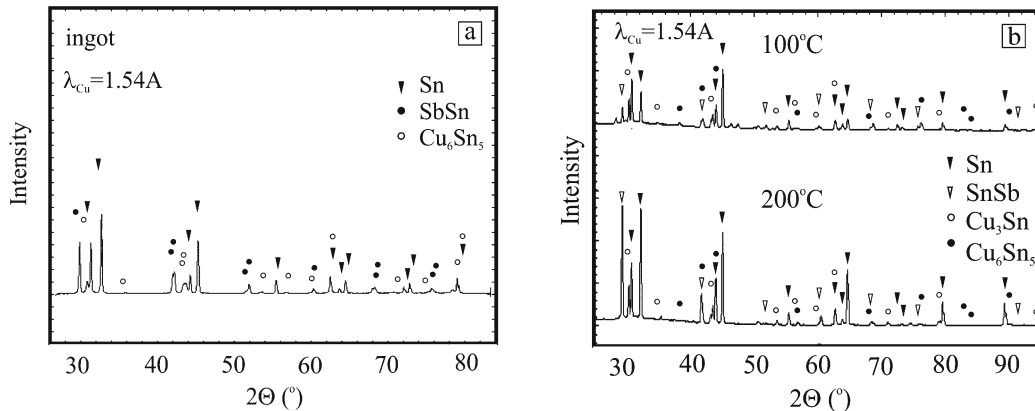


Fig. 8. X-ray diffraction analysis: ingot (a), after annealing (b).

### 3. Results and discussion

Microstructures of the babbitt ingot are presented in Fig. 3, whereas the microstructures after annealing in Figs. 4 and 5. The characteristic hard phases of SnSb (square shape) and CuSn (needle-like shape and spherical shape) on the background of soft matrix rich in tin are observed. The X-ray diffraction presented in Fig. 8 and the chemical composition analysis presented in Figs. 6, 7 confirm occurrence of these phases. Presented in the microstructure precipitates occupy large area of the samples, what can directly influence on the material brittleness. The obtained results are in agreement with the literature data presented in [1, 2].

The grain size of the  $\alpha$ -phase (matrix) in the ingot measure 0.5–1 mm, the  $\beta$ -phase (SnSb) 200  $\mu\text{m}$  and the  $\eta$ -phase (CuSn) 12.5  $\mu\text{m}$ . After annealing, characteristic was recrystallization of the  $\alpha$ -phase – the

measured grain size was in average 200  $\mu\text{m}$  after annealing at 100°C and 250  $\mu\text{m}$  after annealing at 200°C. Both, the  $\beta$ -phase and  $\eta$ -phase, enlarge after annealing at the temperature 100°C. The measured grain size was 235  $\mu\text{m}$  for the  $\beta$ -phase and 15  $\mu\text{m}$  for the  $\eta$ -phase. After annealing at 200°C, an increase of the  $\eta$ -phase amount was characteristic, and some changes of the  $\beta$ -phase shape. The measured grain size after annealing at 200°C was smaller than in ingot and it was: 191  $\mu\text{m}$  for the  $\beta$ -phase and 11  $\mu\text{m}$  for the  $\eta$ -phase.

For a more precise definition of the alloy composition and phase constituents, the chemical composition using EDS analysis and X-ray structure analysis of the alloy was realized. EDS chemical composition analyses presented in Figs. 6 and 7 show that CuSn phase occurs in two morphological forms: needle-like shape and near-spherical shape. These phases probably differ in the stoichiometry – one is  $\text{Cu}_6\text{Sn}_5$  (needle), and the second one is  $\text{Cu}_3\text{Sn}$  (near-spherical shape) (Fig. 8).

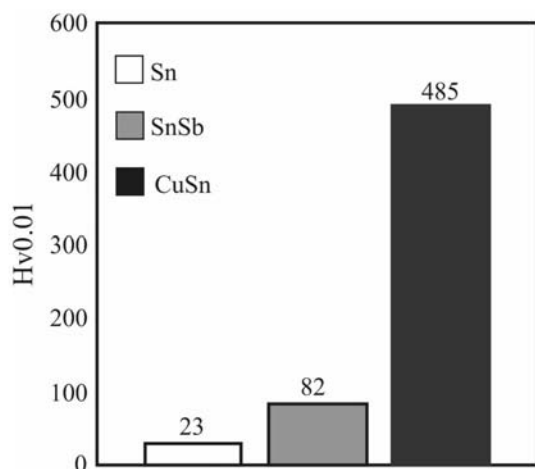


Fig. 9. Microhardness of the SnSbCu babbitt (B83) phases.

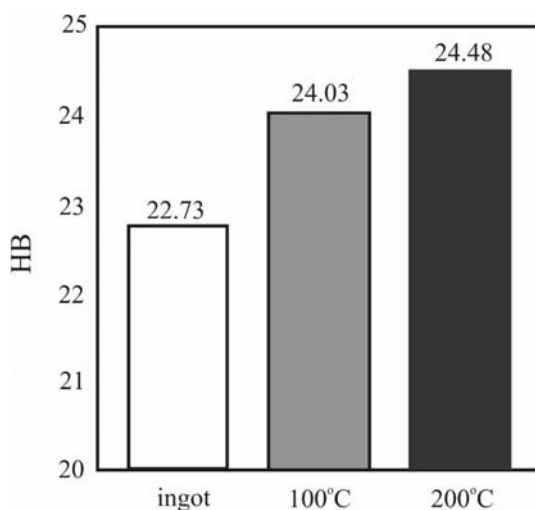


Fig. 10. Hardness of the babbitt alloy.

Presented in Fig. 8 X-ray diffraction analysis of the ingot (Fig. 8a) and the samples after annealing (Fig. 8b) show that after annealing peaks from the  $\alpha$ -phase and the SnSb-phase are higher than in the ingot. The highest peaks are after annealing at the temperature 200°C. Also peaks from the CuSn phase are higher and more numerous after annealing. The peaks from the CuSn phase are weaker than from the  $\alpha$  and SnSb phases.

The results obtained from the microhardness measurements of the phases presented in the SnSb12Cu6Pb alloy are given in Fig. 9, whereas the hardness measurements in Fig. 10. The microhardness was measured using small load 10 g. Small load makes it possible to measure each phase presented in the alloy. The highest average value of the microhardness has CuSn phase, the microhardness is equal to 485 HV0.01. The microhardness of the SnSb phase (in the form of the

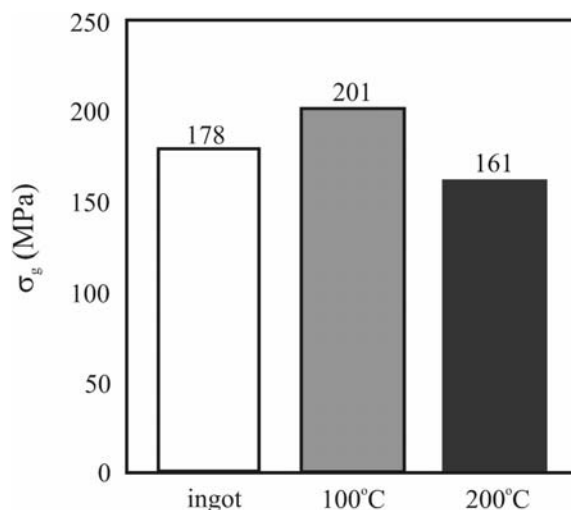


Fig. 11. The comparison of the bending strength of cast and annealed babbitt alloy.

squares) was found to be six times smaller and equal to 82 HV0.01. The average microhardness of the matrix ( $\alpha$ -phase) was about 23 HV0.01 (Fig. 9).

With the exception of the CuSn phase, results of the microhardness measurements are comparable with the data presented by Sadykov et al. [6]. The differences could result from the small size of the CuSn phase and load used in the measurements.

Results of the hardness measurements show higher level of the properties after annealing. The average value is near 23 HB and 24.5 HB for the babbitt ingot and annealed samples, respectively (Fig. 10).

The highest level of the hardness after annealing, especially at the temperature 200°C, could result in the higher amount of the fine CuSn phase distributed uniformly in the tin matrix. As was presented in Fig. 8b, after annealing, peaks from the CuSn phase are sharply outlined in contrast to the babbitt ingot. Additionally, this was confirmed by microstructure observations and shown in Figs. 3–5.

The results obtained in the bending test (Fig. 11) show the highest bending strength in the sample annealed at 100°C in comparison to the ingot babbitt and sample annealed at 200°C. The mean value of the bending strength was 201 MPa for the sample annealed at the 100°C and 178 MPa for the ingot babbitt. The smallest value of the bending strength demonstrates a sample annealed at the temperature  $T_a = 200^\circ\text{C}$ : 161 MPa.

Fractures presented in Figs. 12–14 prove that crackings nucleate and propagate mainly through the hard phases both in ingot babbitt and annealed samples. The analysis of the cracks indicates fractures of the SnSb ( $\beta$ ) and CuSn ( $\eta$ ) hard phases and ductile fracture of the tin ( $\alpha$ -phase) (Figs. 12–14). The low ductility of babbitt alloy is caused mainly by brittle-

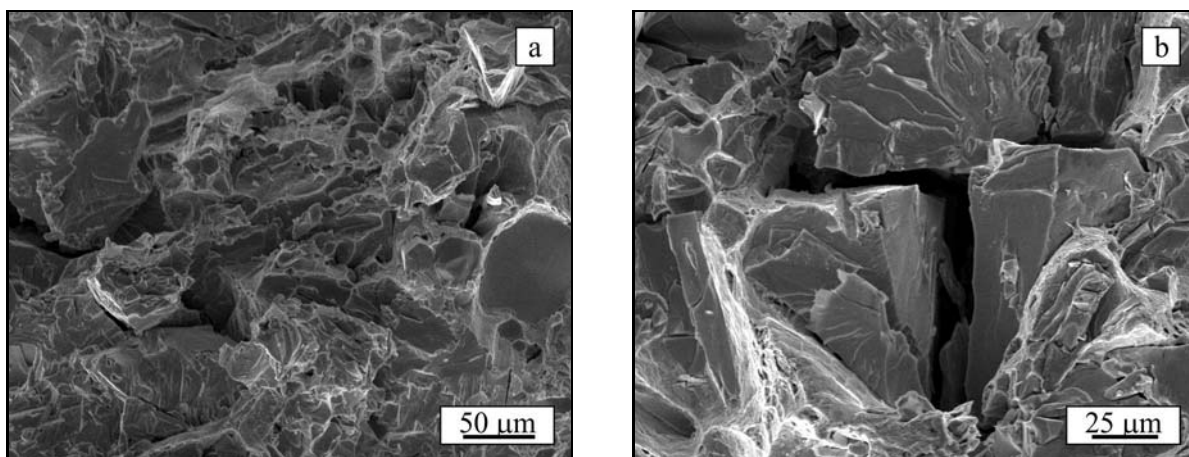


Fig. 12a,b. Scanning electron micrographs of destroyed babbitt surface; ingot of babbitt alloy.

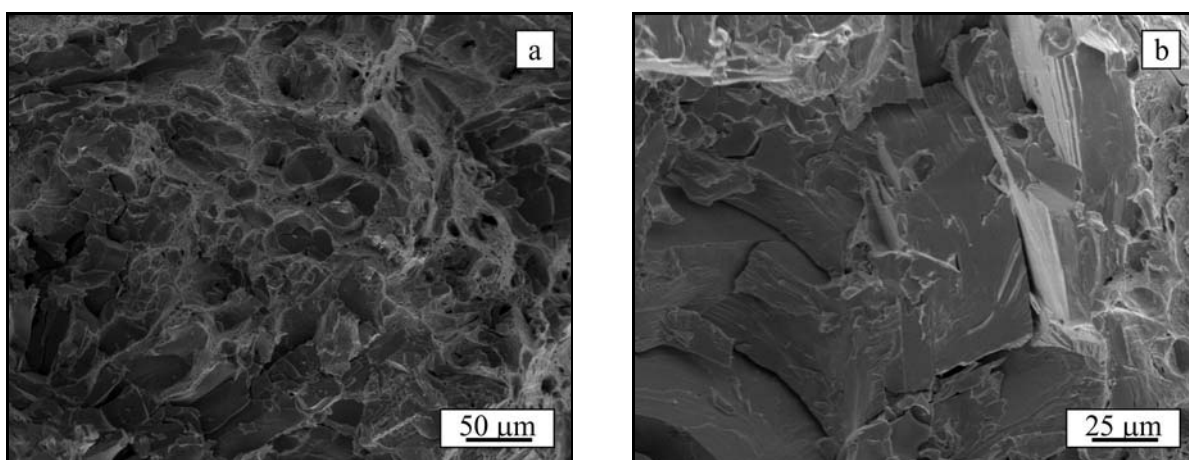


Fig. 13a,b. Scanning electron micrographs of destroyed annealed babbitt surface;  $T_a = 100\text{ }^\circ\text{C}$ ,  $t = 2\text{ h}$ .

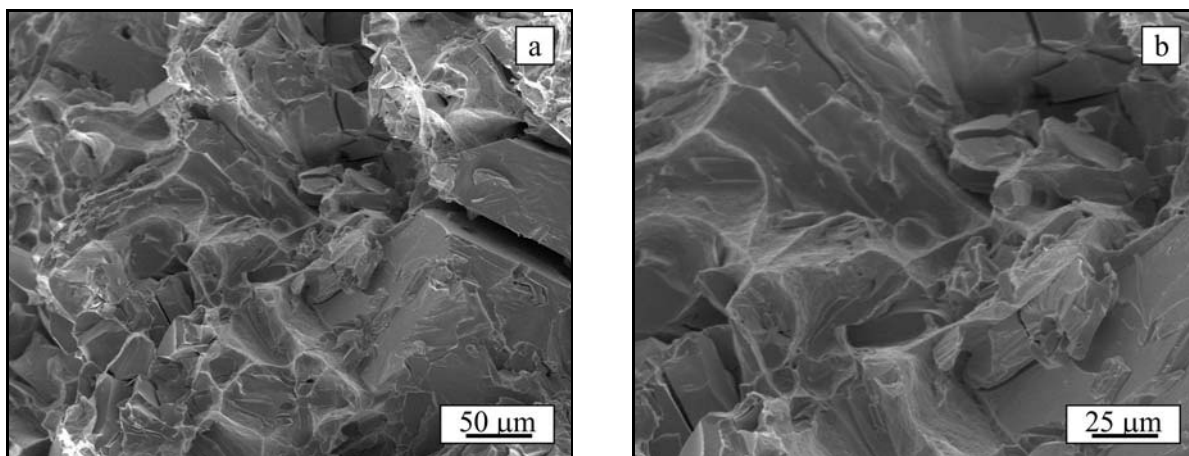


Fig. 14a,b. Scanning electron micrographs of destroyed annealed babbitt surface;  $T_a = 200\text{ }^\circ\text{C}$ ,  $t = 2\text{ h}$ .

ness of the  $\beta$ -phase, which because of the hexagonal lattice has a limited number of slip planes available for plastic deformation [6].

The babbitt samples were used for wear tests per-

formed by the block-on-ring wear tester. The results are presented as graphs of the mass loss (Fig. 15) and friction coefficient (Fig. 16) in dependence on the sliding distance.

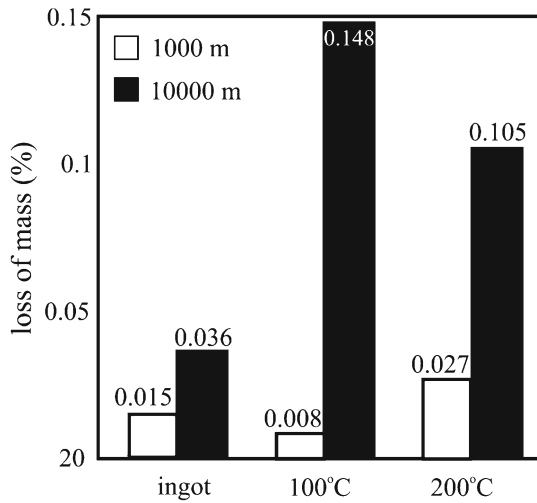


Fig. 15. Dependence of the sliding distance: 1000 m and 10000 m on the loss of mass of babbitt alloy in wet test.

The loss of mass is a measure of the tribological properties of the babbitt samples. By comparing the wear resistance of samples received from ingot and annealed babbitt samples, it is evident that the babbitt ingot after sliding on a distance of 1000 m shows almost 2 times lower loss of mass than the sample from the babbitt annealed at 200 °C. The babbitt ingot after sliding on a distance of 10000 m shows more than 3 times lower loss of mass than the samples from the babbitt annealed at 200 °C and near 4 times lower loss of mass than the samples from the babbitt annealed at 100 °C. The presence of easily spalling coarse  $\beta$ -phase particles is responsible for the low wear resistance of babbitt. It is known that refinement of the  $\beta$ -phase has a positive effect on the fatigue strength and wear resistance of babbitt bushes. It is clear that the abrasive wear resistance of babbitt samples against steels with dispersed carbides also increased with increasing

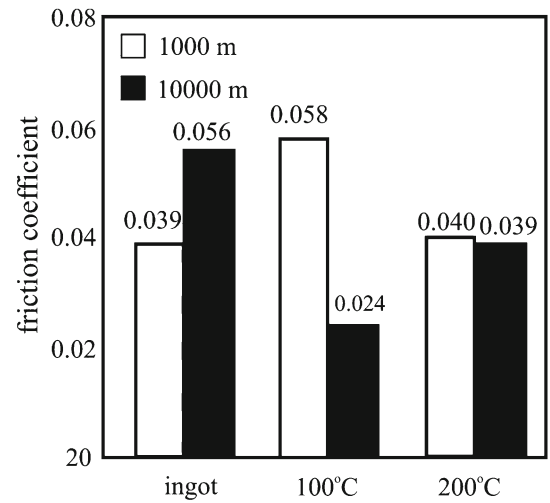


Fig. 16. Dependence of the sliding distance: 1000 m and 10000 m on the friction coefficient of babbitt alloy in wet test.

tin matrix ( $\alpha$ ) volume content. The highest level of the loss of mass after annealing, especially at temperature 100 °C after 10000 m sliding distance, can result in the higher amount of the fine hard CuSn phase distributed uniformly in the tin matrix and  $\beta$ -phase grain growth during annealing. As was presented in Fig. 8b, after annealing, peaks from the CuSn phase are sharply outlined in opposition to the babbitt ingot. So the role of the tin matrix during tribological test in the annealed babbitt samples was lower in comparison to babbitt ingot. The  $\eta$ (CuSn) phases seen on the wear-surfaces are being crushed and pulled out of the matrix to act as abrasive particles which increase the loss of mass of annealed samples. Carbides  $\text{Cr}_{23}\text{C}_6$  from steel 100Cr6 and CuSn abrasives are known to easily penetrate the soft tin matrix during sliding, which results in excessive material removal from the worn surface of babbitt. Figure 17 shows smearing of tin over the surface

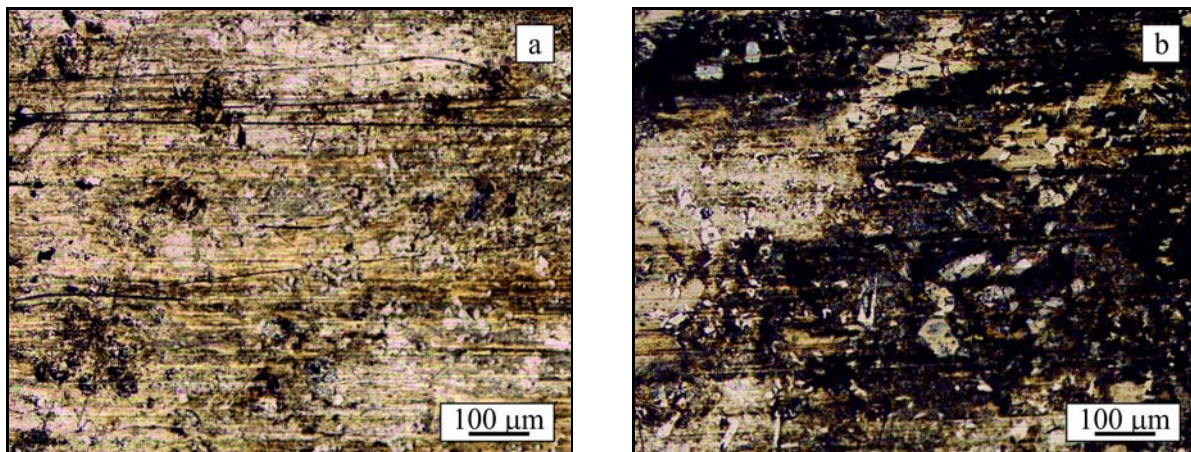


Fig. 17. The surface of the babbitt ingot after examining the wear resistance on 1000 m (a) and 10000 m (b) distance.

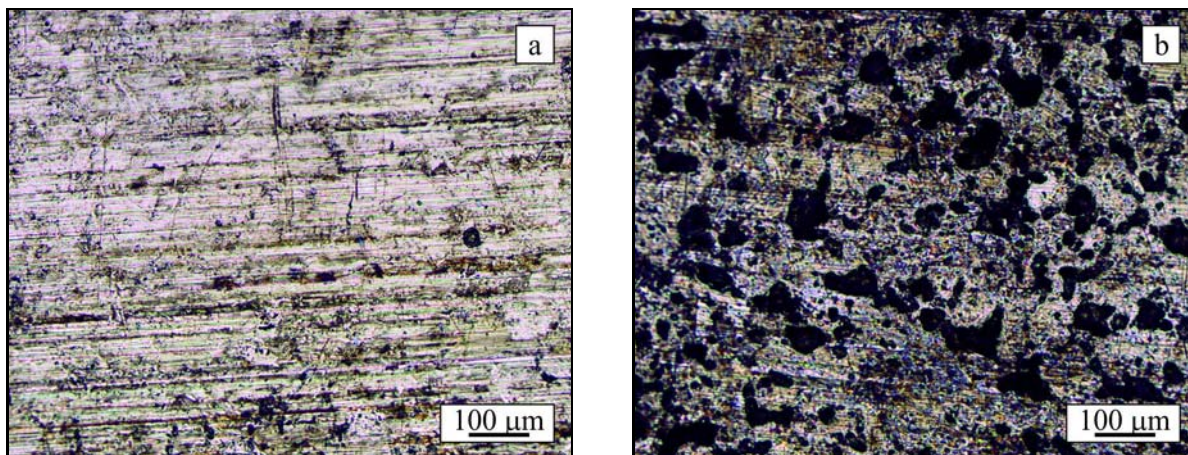


Fig. 18. The surface of the annealed at 100°C babbitt after examining the wear resistance on 1000 m (a) and 10000 m (b) distance.

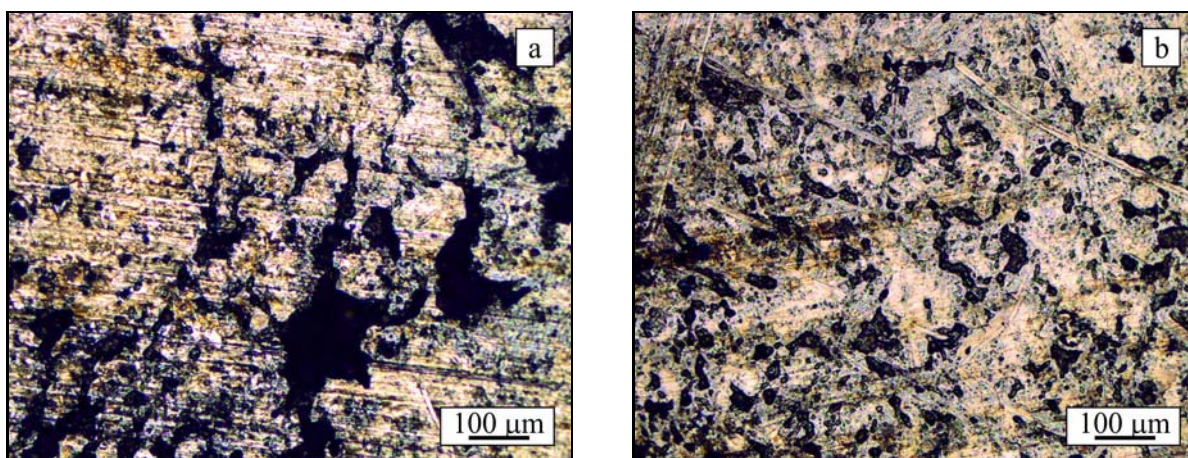


Fig. 19. The surface of the annealed at 200°C babbitt after examining the wear resistance on 1000 m (a) and 10000 m (b) distance.

of babbitt ingot which results in the smallest loss of mass after 1000 m and 10000 m sliding distance in comparison to annealed samples.

An application of oil TU 32 as a lubricant and simultaneously as a cooling-separating medium causes a decrease of the friction coefficient [8]. A friction coefficient value of over 0.01 in lubricant oil, in general, means that oil films are partially or discontinuously formed at the interface between the friction material and the mating material. From these viewpoints, the above results seem to indicate that stable lubricant oil films were not formed at the sliding interface between the babbitt and steel samples. From Fig. 16 it is evident that the friction coefficient of annealed babbitt is approximately equal to the friction coefficient of babbitt alloy, whereas the annealing of babbitt at 100°C has a negligible effect on the friction coefficient.

Characteristic surface topographies after the wear test are presented in Figs. 17–19.

There were found some scratches, microploughings

and small seizure areas. The scratches and seizure cause a high friction coefficient. In the babbitt after examining the wear resistance on 10000 m distance shown in Figs. 17b, 18b, 19b, some deep scratches and holes were observed on the sliding surface, which corresponded to traces of  $\beta$ -phase particles detached from the matrix. There is a fresh surface also observed. The detached  $\text{SnSb}(\beta)$  and  $\text{CuSn}(\eta)$  particles seem to cause abrasive wear or seizure phenomena. As it could be seen in Figs. 17a, 18a, 19a (1000 m), the cutting efficiency of the fine abrasive  $\text{CuSn}(\eta)$  particles decreased to a great extent, because the abrasive produced shallower cuts on the specimen surface, forming shallow grooves only.

#### 4. Conclusion

The main object of this study was to determine the influence of the heat treatment on the microstructure

and properties of the bearing babbitt SnSb12Cu6Pb. It is evident that the annealing of babbitt results in microstructural changes. After annealing, characteristic was recrystallization of the  $\alpha$ -phase – the measured grain size was in average 200  $\mu\text{m}$  after annealing at 100 °C and 250  $\mu\text{m}$  after annealing at 200 °C. Both the  $\beta$ -phase and  $\eta$ -phase grew after annealing at the temperature 100 °C. The measured grain size was 235  $\mu\text{m}$  for the  $\beta$ -phase and 15  $\mu\text{m}$  for the  $\eta$ -phase. EDS chemical composition analyses presented in Figs. 6 and 7 showed that CuSn phase occurred in two morphological forms: needle-like shape ( $\text{Cu}_6\text{Sn}_5$ ) and near-spherical shape ( $\text{Cu}_3\text{Sn}$ ).

Results of the hardness measurements show higher level of the properties in the samples after annealing. The average value was near 23 HB and 24.5 HB for the babbitt ingot and annealed samples. The results obtained in the bending test show highest bending strength in the sample annealed in the 100 °C in comparison to the ingot babbitt and sample annealed at 200 °C. By comparing the wear resistance of samples received from ingot and annealed babbitt samples, it is evident that the babbitt ingot after sliding on a distance of 1000 m and 10000 m shows lower loss of mass than the samples from the babbitt annealed at 100 °C and 200 °C. It is mainly affected by the presence of easily spalling coarse bigger  $\beta$ -phase particles in the microstructure of annealed babbitt.

## References

- [1] Khrushchev, M. M., Kuritsyna, A. D.: Friction and Wear in Machines, 5, 1950, p. 76 (in Russian).
- [2] Barykin, N. P., Sadykov, F. A., Aslanyan, I. R.: Journal of Materials Engineering and Performance, 2, 2000, p. 127.
- [3] Barykin, N. P., Sadykov, F. A., Aslanyan, I. R.: Trenie Iznos, 21, 2000, p. 634.
- [4] Potekhin, B. A., Il'yushin, V. V., Khristolyubov, A. S.: Metal Science and Heat Treatment, 51, 2009, p. 378. [doi:10.1007/s11041-009-9181-1](https://doi.org/10.1007/s11041-009-9181-1)
- [5] PN-ISO 4381:1997.
- [6] Sadykov, F. A., Barykin, N. P., Valeev, I. Sh., Danilenko, V. N.: Journal of Materials Engineering and Performance, 12, 2003, p. 29. [doi:10.1361/105994903770343448](https://doi.org/10.1361/105994903770343448)
- [7] Leszczyńska-Madej, B., Madej, M.: Archives of Metallurgy and Materials, 56, 2011, p. 805.
- [8] Madej, M., Leszczyńska-Madej, B., Koza, J.: Rudy i Metale Nieżelazne, 56, 2011, p. 288 (in Polish).
- [9] Predel, B.: Phase equilibria, crystallographic and thermodynamic data of binary alloys. Vol. 5. Berlin Heidelberg, Springer-Verlag 1998.